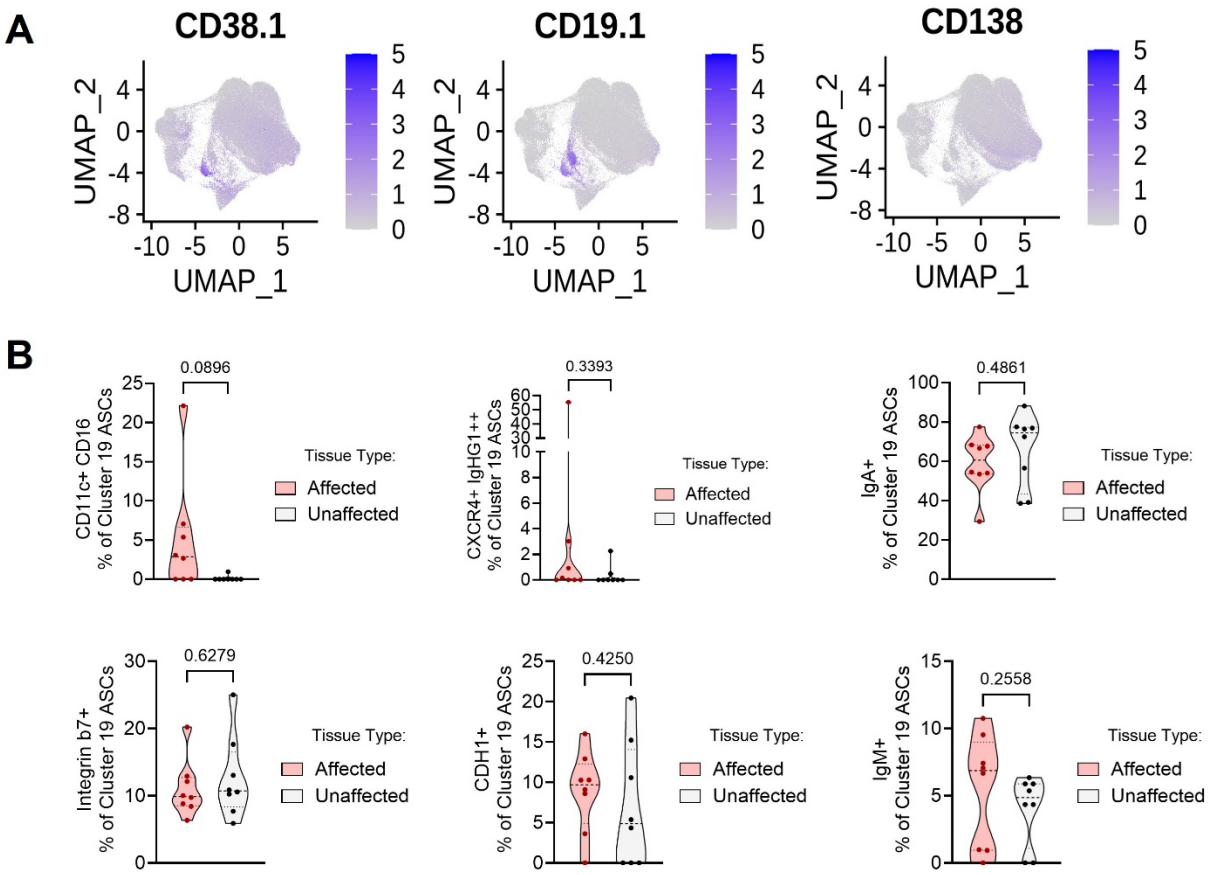
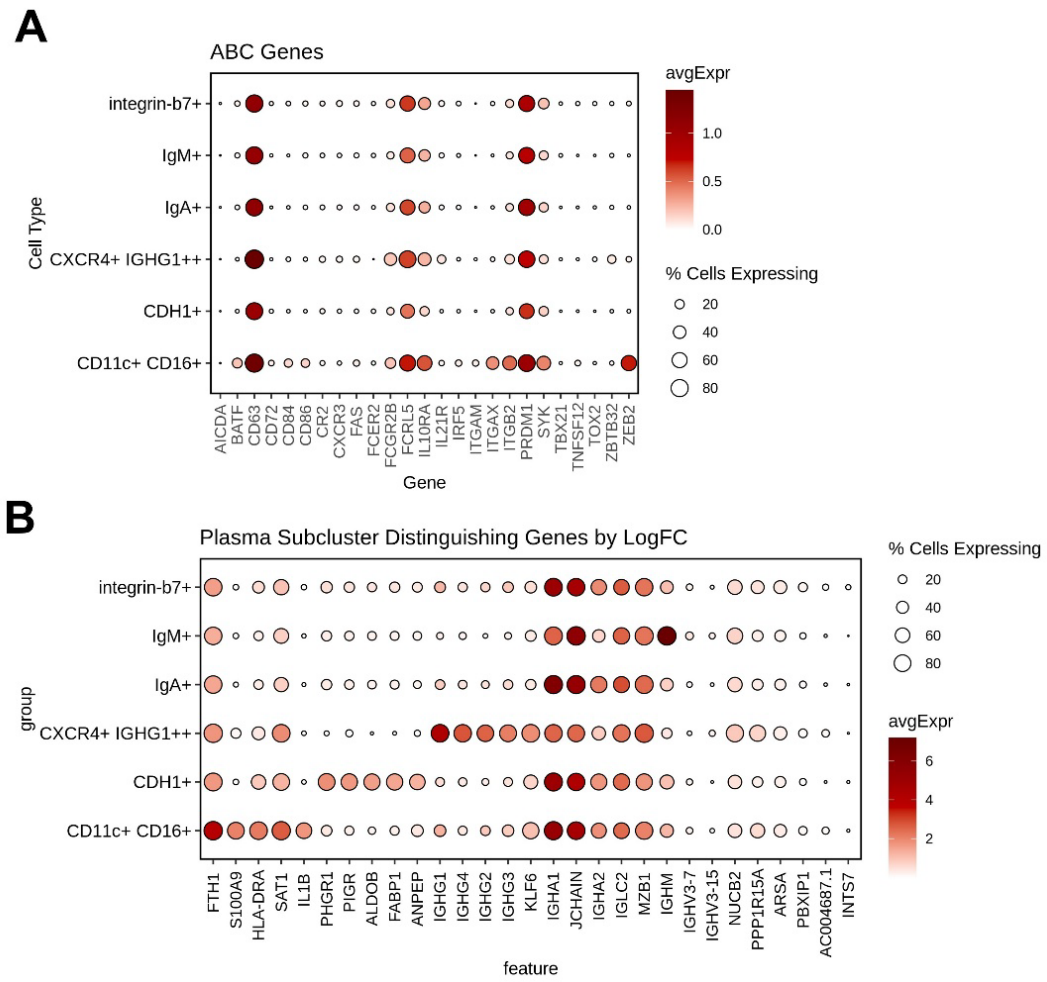
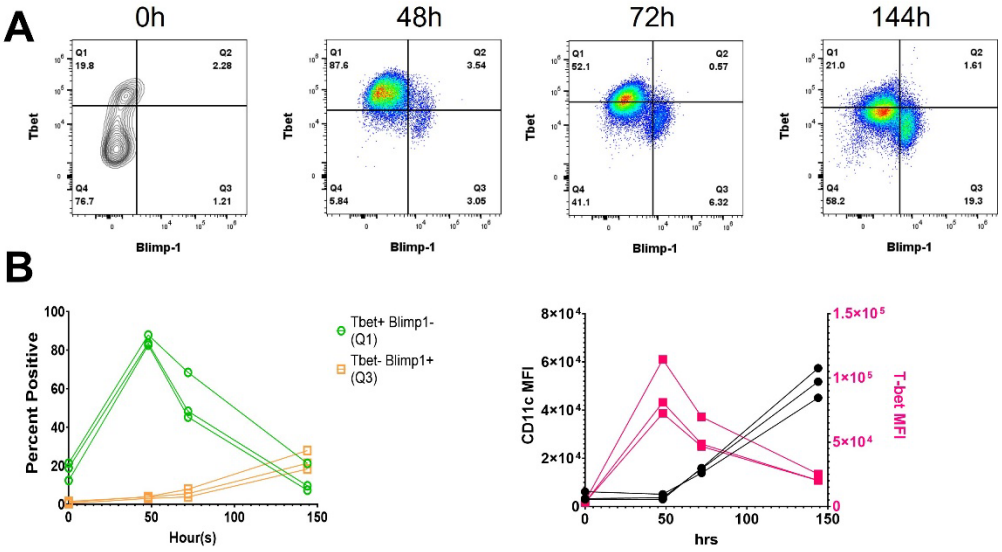


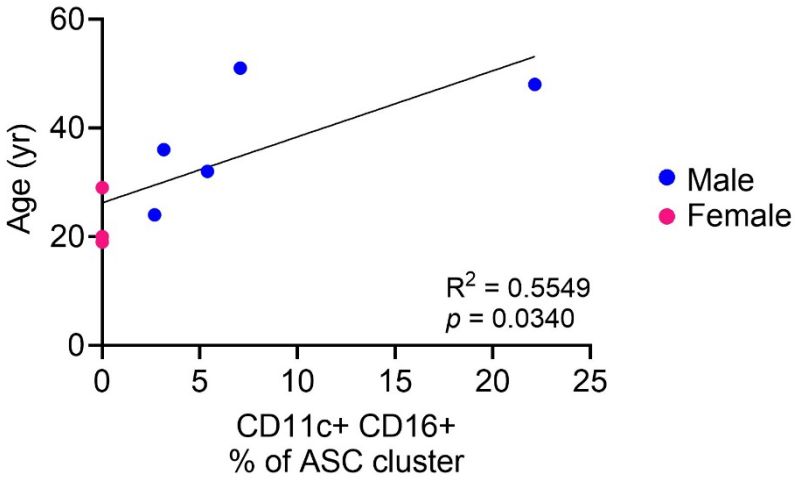
Supplemental Figure 1: ASC marker expression and relative abundance of ASC sub-populations in affected/unaffected tissue resections from Crohn's disease patients**. (A)** Surface protein expression of CD38, CD19, and CD138 in annotated cell clusters from Figure 1B. Color intensity shows expression intensity by log normalized ADT. **(B)** Relative abundance (percentage within cluster) of the CD19+ ASC subpopulations defined in Figure 1E. Statistics were analyzed by paired Student's t test and were nonsignificant.



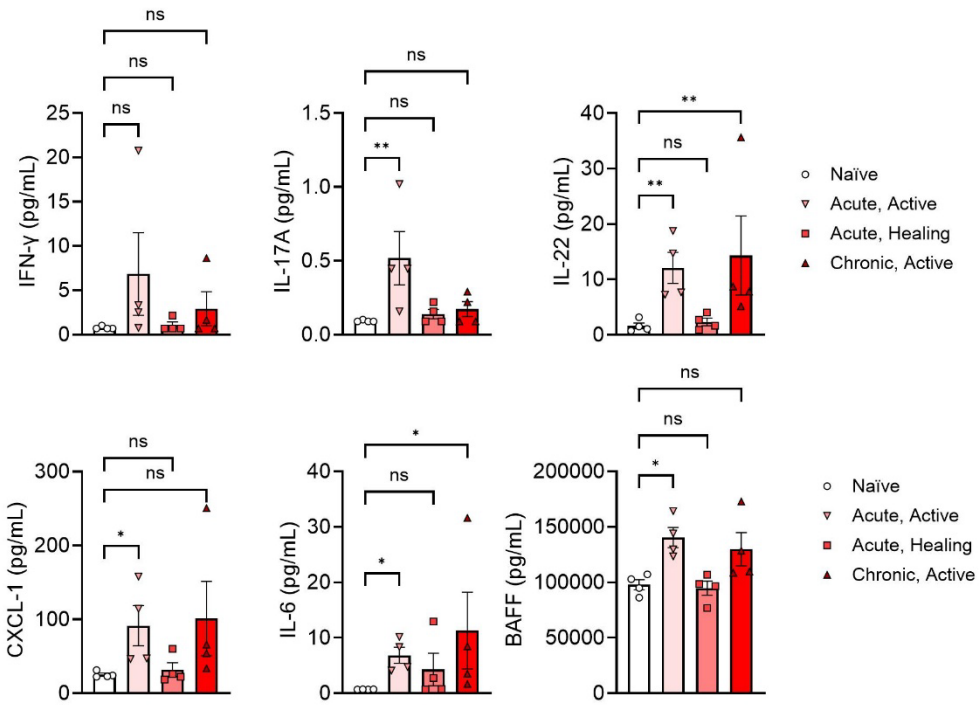
Supplemental Figure 2: Key transcript expression in CD19+ ASCs from CD patient resections. **(A)** Expression patterns of key genes associated with ABC phenotypes from CD19+ ASC subclusters. **(B)** Expression patterns of the top five genes which distinguish each subcluster from the others. Bubble size reflects the percentage of cells within the cluster expressing each gene, color reflects average expression.



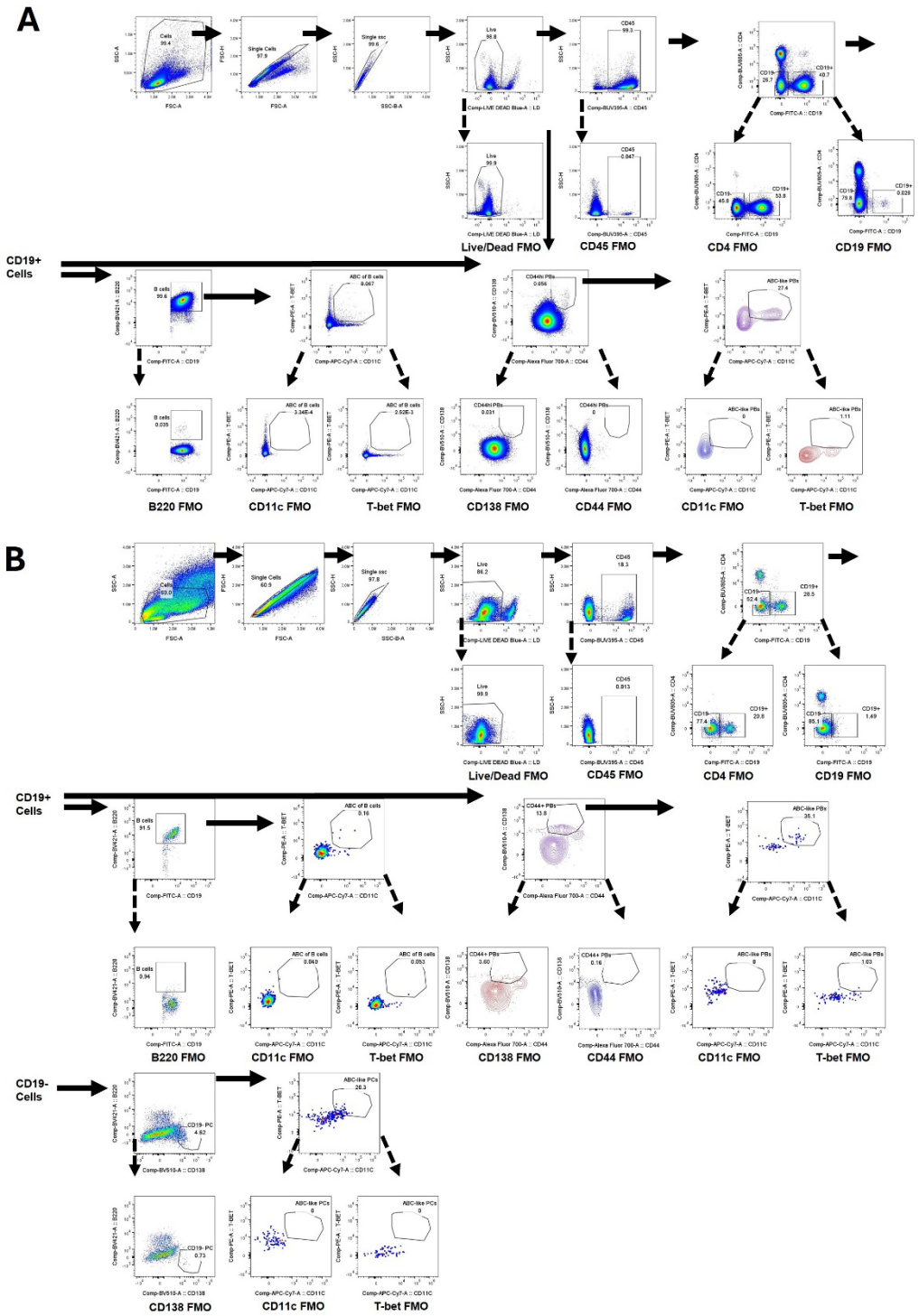
Supplemental Figure 3: T-bet is lost in human ABCs over time *in vitro* as Blimp-1 emerges. **(A)** Representative flow plots of human isolated B cells cultured in an ABC-stimulating condition (R848, IL-21, IFN-γ, CD40L, anti-IgM) over 6 days in culture. Plots show T-bet versus Blimp1 expression. **(B)** Expression of T-bet, Blimp1, and CD11c in stimulated B cells represented as % of total cells or MFI. Data is from one experiment with B cells derived from 3 healthy donors. In **B**, dots represent individual donors and lines connect each time point per donor.



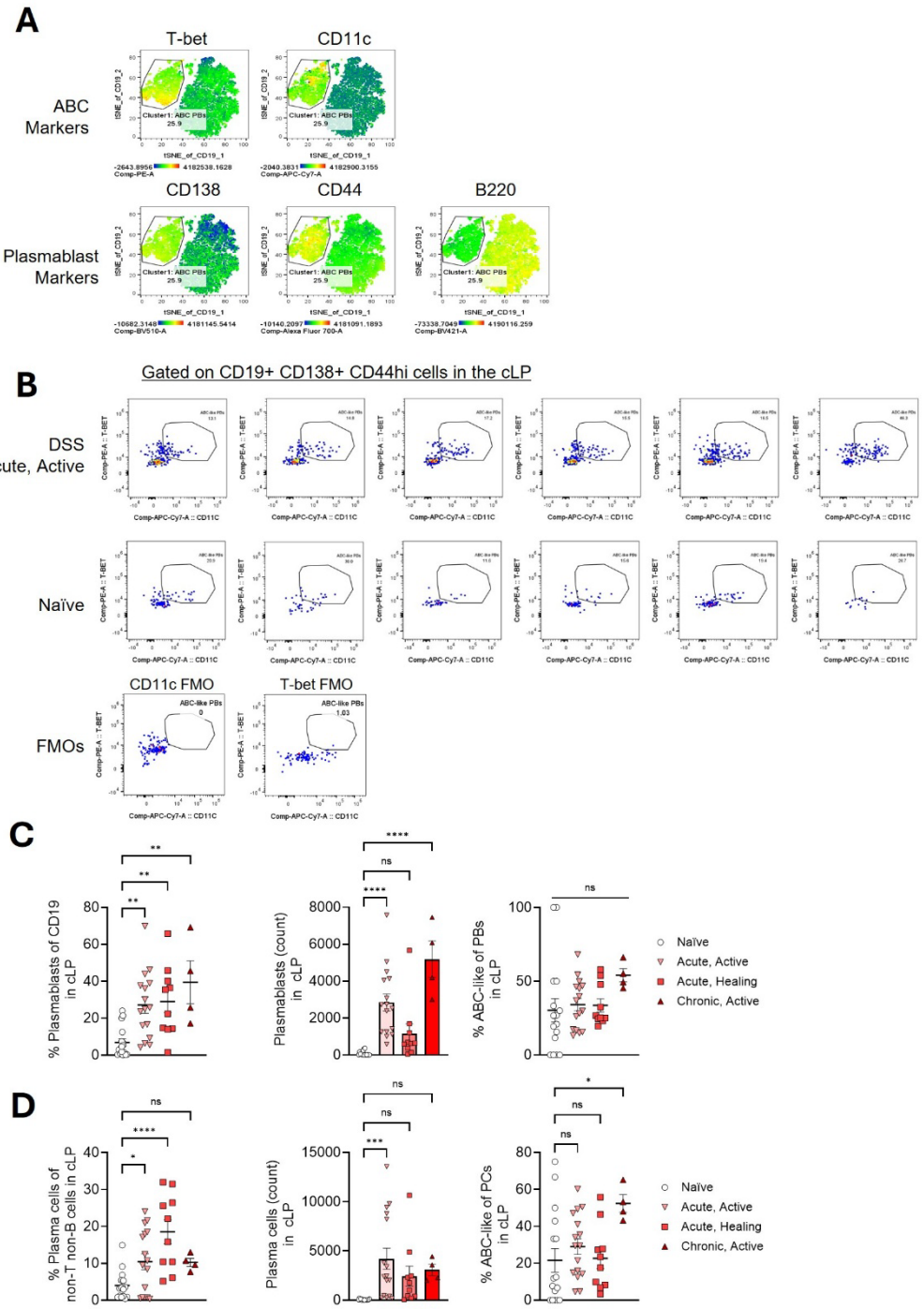
Supplemental Figure 4: Correlation of CD11c+ ASC abundance versus patient age at time of resection. Correlation was analyzed by simple linear regression and statistics are shown on the plot.



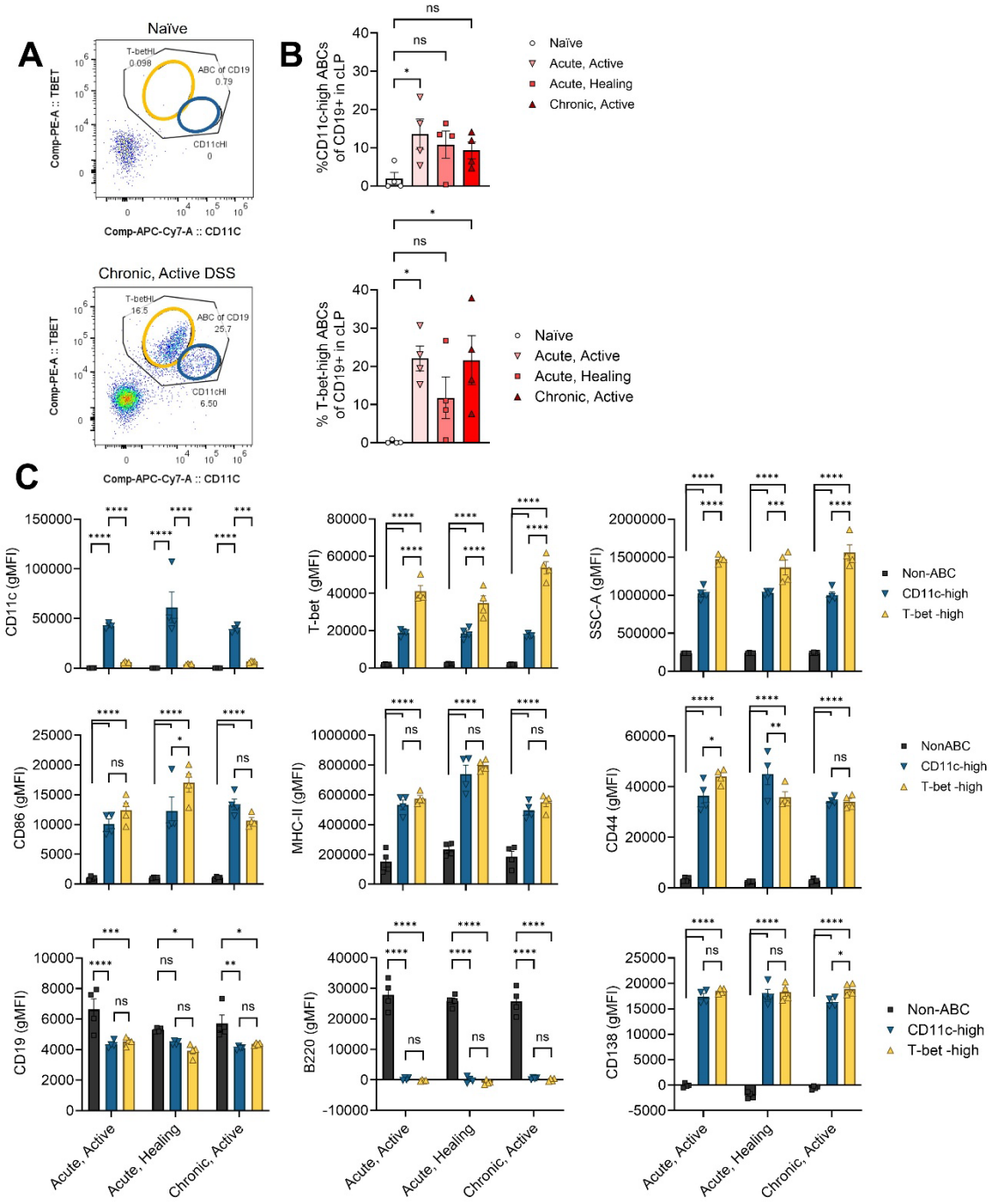
Supplemental Figure 5: Serum cytokines are elevated in DSS-treated mice following acute and chronic exposure. Serum cytokines were measured by LegendPlex assay. Data was generated from one experiment and statistics were analyzed by lognormal One-Way ANOVA with Dunnett's multiple comparison's test against the naïve group. *P < 0.05, ** P < 0.01. ns: nonsignificant.



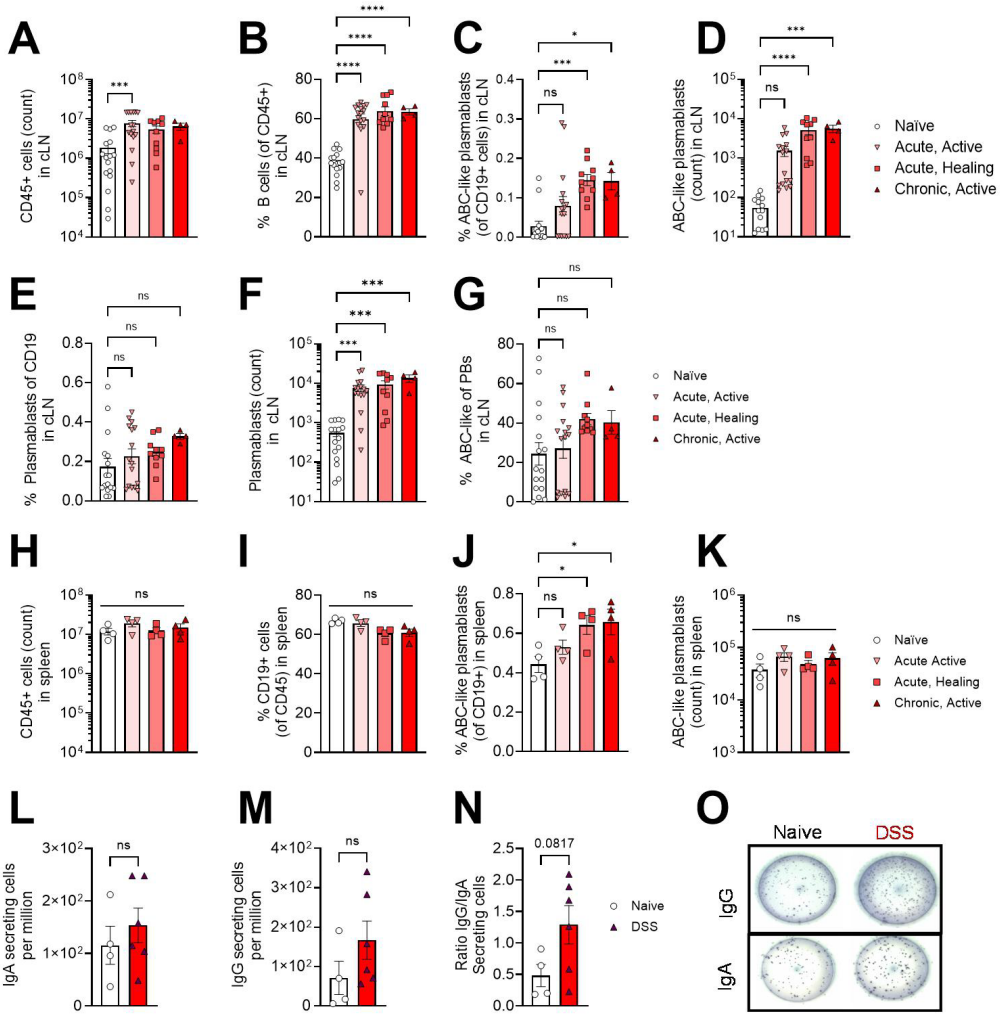
Supplemental Figure 6: Gating strategies for in vivo experiments. Gating strategy is shown for the colon-draining lymph node **(A)** and colon lamina propria **(B)** with fluorescence minus one (FMO) controls.



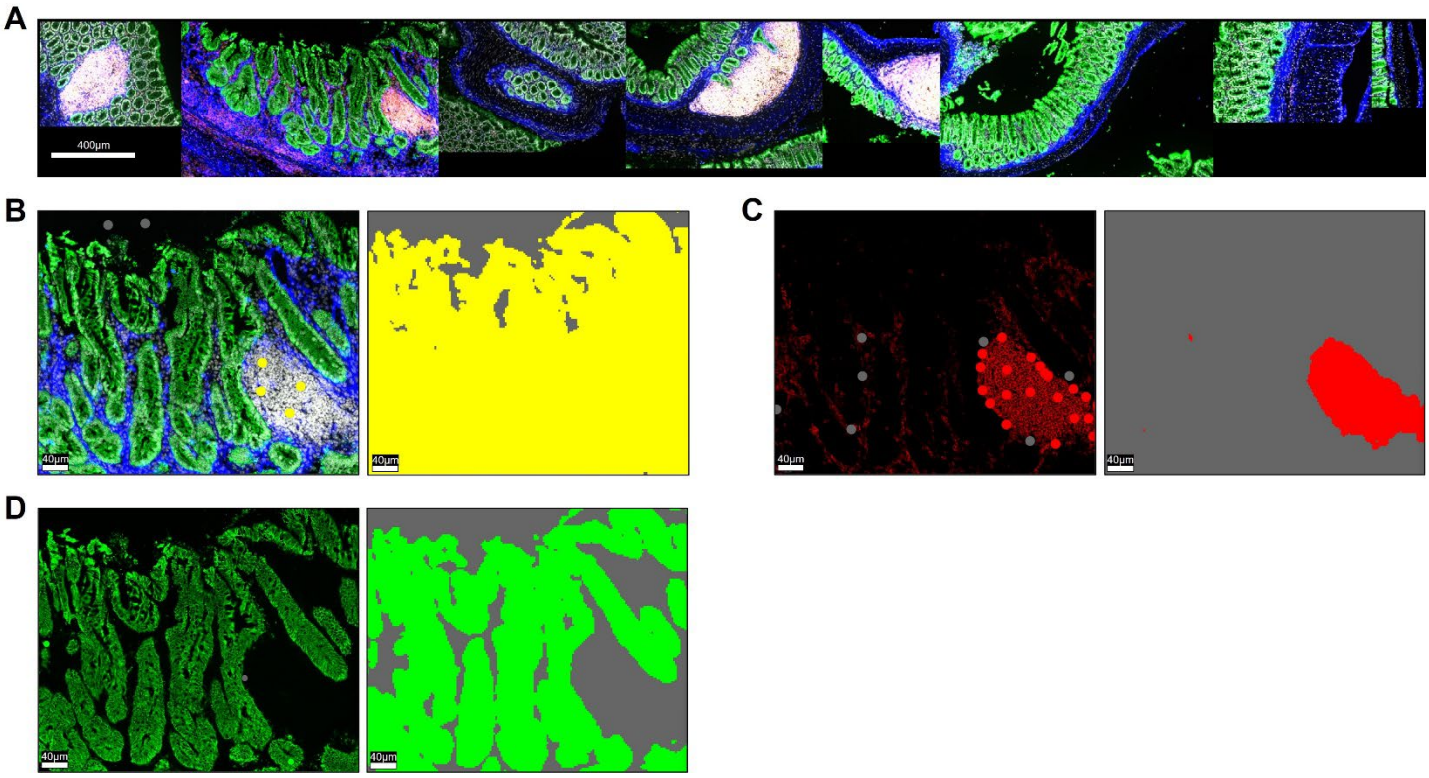
Supplemental Figure 7: Plasmablast and ABC-like plasmablast populations in the colon lamina propria (cLP). **(A)** tSNE plot of CD19$^+$ cells from the colon LP of a DSS-treated mouse. A cluster of ABC-like plasmablasts is circled, and colors represent expression patterns of markers associated with ABCs (T-bet, CD11c) and plasmablasts (CD138, CD44, B220). **(B)** Representative flow cytometry plots of ABC markers (CD11c, T-bet) among plasmablasts in the cLP. Each plot is from an individual mouse or shows FMO controls. **(C)** Plasmablasts as percent of CD19$^+$ cells, number of plasmablasts, and percentage of ABC-like cells among plasmablasts (PBs) in the cLP. **(D)** Plasma cells as percent of non-T and non-B cells (CD19-, CD3-), number of plasma cells, and percentage of ABC-like cells among plasma cells (PCs) in the cLP. Data is pooled from 3 experiments and corresponds to the data shown in Figure 2. Statistics are analyzed by One-Way ANOVA with Dunnett's multiple comparison's test against the naïve group. Points represent individual mice, bars represent mean ± s.e.m. *P < 0.05, **P < 0.01, ***P < 0.001, ****P < 0.0001. ns: nonsignificant.



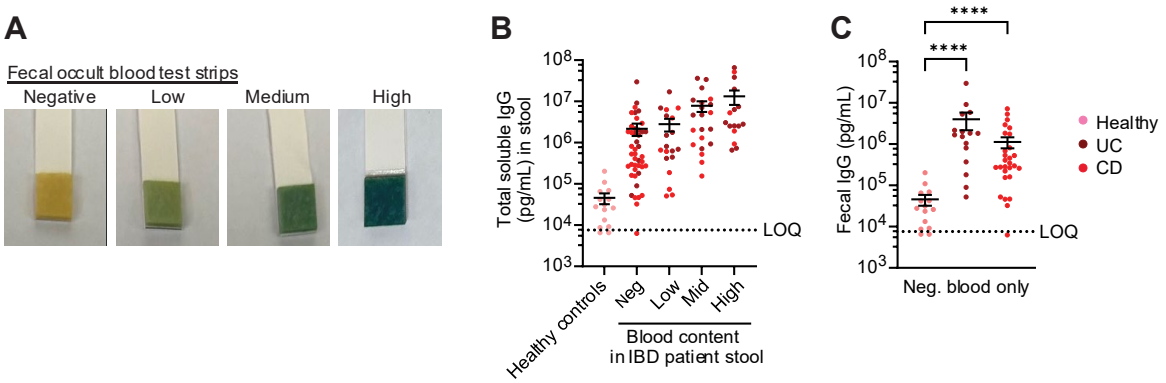
Supplemental Figure 8: ABC sub-populations among CD19⁺ cells in the colon LP of DSS-treated mice. **(A)** Representative flow plots of ABCs among CD19⁺ cells in the colon LP demonstrating a T-bet high population (yellow) and a CD11c high population (blue). **(B)** Relative abundance of T-bet high ABCs and CD11c high ABCs from the colon LP. **(C)** Key marker expression (gMFI) and side scatter (SSC-A) of ABC subpopulations and non-ABCs from the colon LP of DSS-treated mice at various timepoints. Data is from one of three experiments related to Figure 2. Statistics were analyzed by One-Way ANOVA with Dunnett's multiple comparison's test against the naïve group **(B)** or two-way ANOVA with Sidak's multiple comparisons test **(C).** For bar graphs, points represent individual mice, bars represent mean ± s.e.m. **P* < 0.05, ***P* < 0.01, ****P* < 0.001, *****P* < 0.0001. ns: nonsignificant.



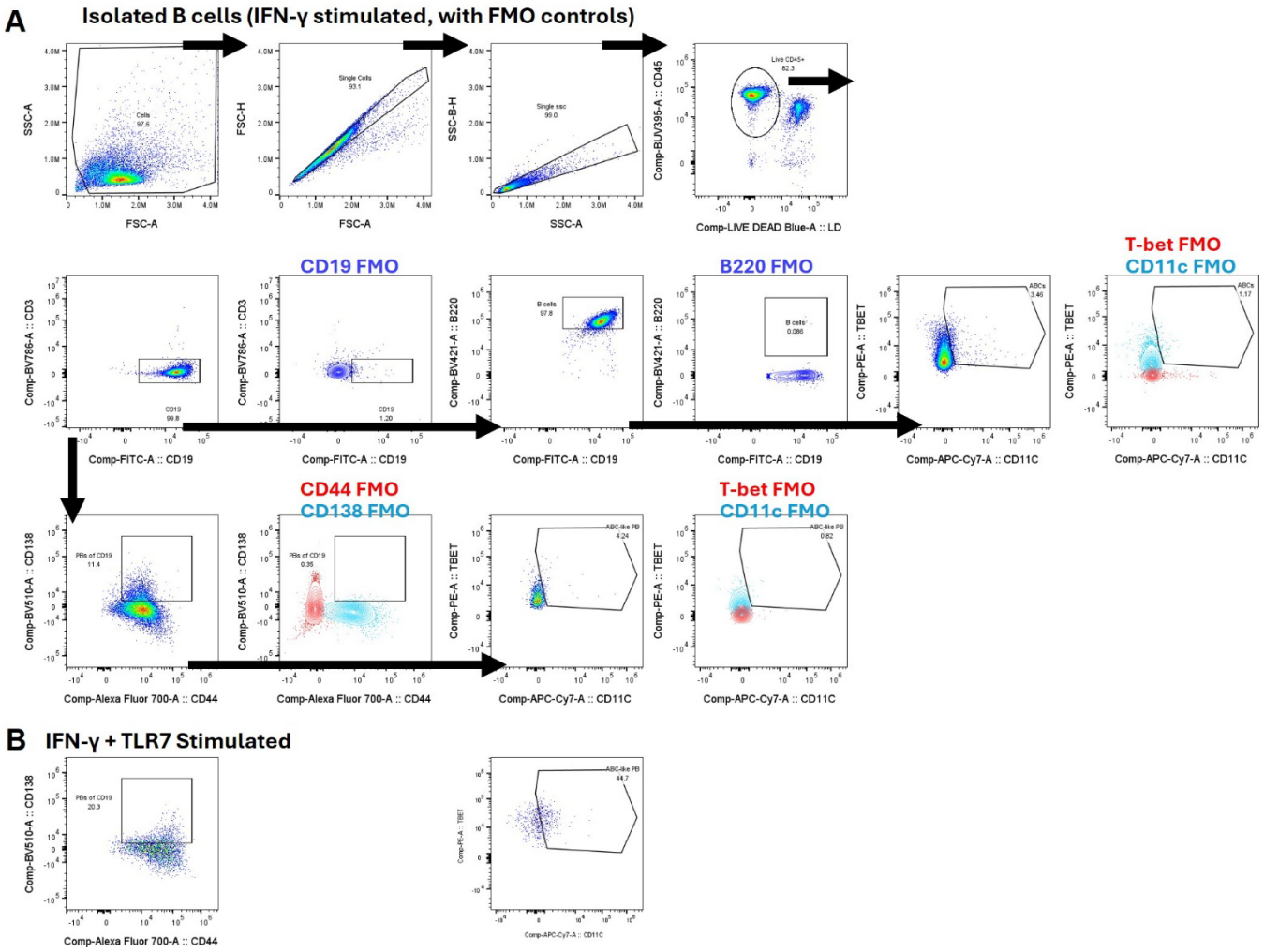
Supplemental Figure 9: B cells expand in the cecal-colonic lymph node after DSS injury, but splenic B cells are generally unchanged. **(A-G)** Abundance of total CD45+ cells (**A**), B cells (**B**), ABC-like plasmablasts (**C, D, G**), and total plasmablasts (**E, F**) in the cecal-colonic lymph node (cLN) measured by flow cytometry. Cell populations are represented as total counts or percentages of parent population. **(H-K)** Abundance of total CD45+ cells (**H**), CD19+ cells (**I**), and ABC-like plasmablasts (**J, K**) in the spleen. **(L-O)** Abundance (number per million live cells) of IgA (**L**) and IgG (**M**) secreting cells and the ratio of IgG to IgA secreting cells per mouse (**N**) in the cLN measured by ELISpot. **(O)** Representative image of ELISpots from the cLN. cLN flow cytometry data is pooled from 3 independent experiments (**A-G**). Spleen flow cytometry was from 1 experiment (**H-K**), ELISpots were from 1 representative experiment of 2 (**L-O**). Statistics were analyzed by one-way ANOVA with Dunnett's multiple comparison's test against the naïve group (**A-K**) or Student's t test (**L-N**). For bar graphs, points represent individual mice, bars represent mean ± s.e.m. **P* < 0.05, ***P* < 0.01, ****P* < 0.001, *****P* < 0.0001. ns: nonsignificant.



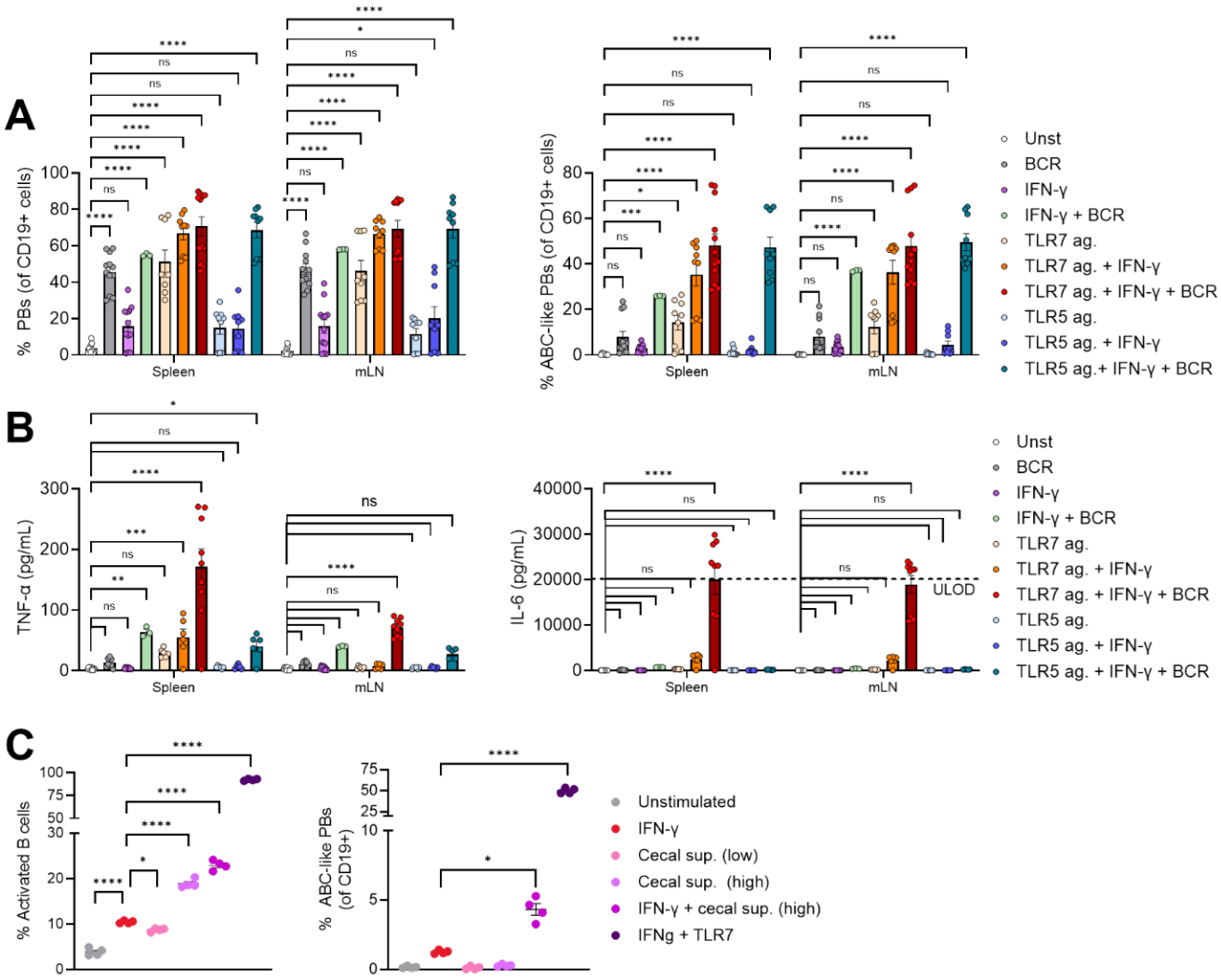
Supplemental Figure 10: Tissue pixel classifiers related to Figure 2. **(A)** Screenshot of composite image used to train pixel classifiers. **(B)** Example staining of DAPI (white), CD90.2 (blue), and EpCam (green) staining with negative (grey) and positive (yellow) training points. Resultant tissue mask (yellow) is shown to the right, which was used with a minimum object size of 100 μm^2 and minimum hole size of 1000 μm^2 to create tissue annotation. **(C)** Example staining of CD45 (red) staining with negative (grey) and positive (red) training points. Resultant tissue mask (red) is shown to the right, which was applied within the tissue annotation with a minimum object size of 2500 μm^2 and minimum hole size of 1000 μm^2 to create tissue annotation. **(D)** Example staining of EpCam (green) staining with negative (grey) and positive (green) training points. Resultant tissue mask (green) is shown to the right, which was applied within the tissue annotation with a minimum object size of 100 μm^2 and minimum hole size of 1000 μm^2 to create tissue annotation.



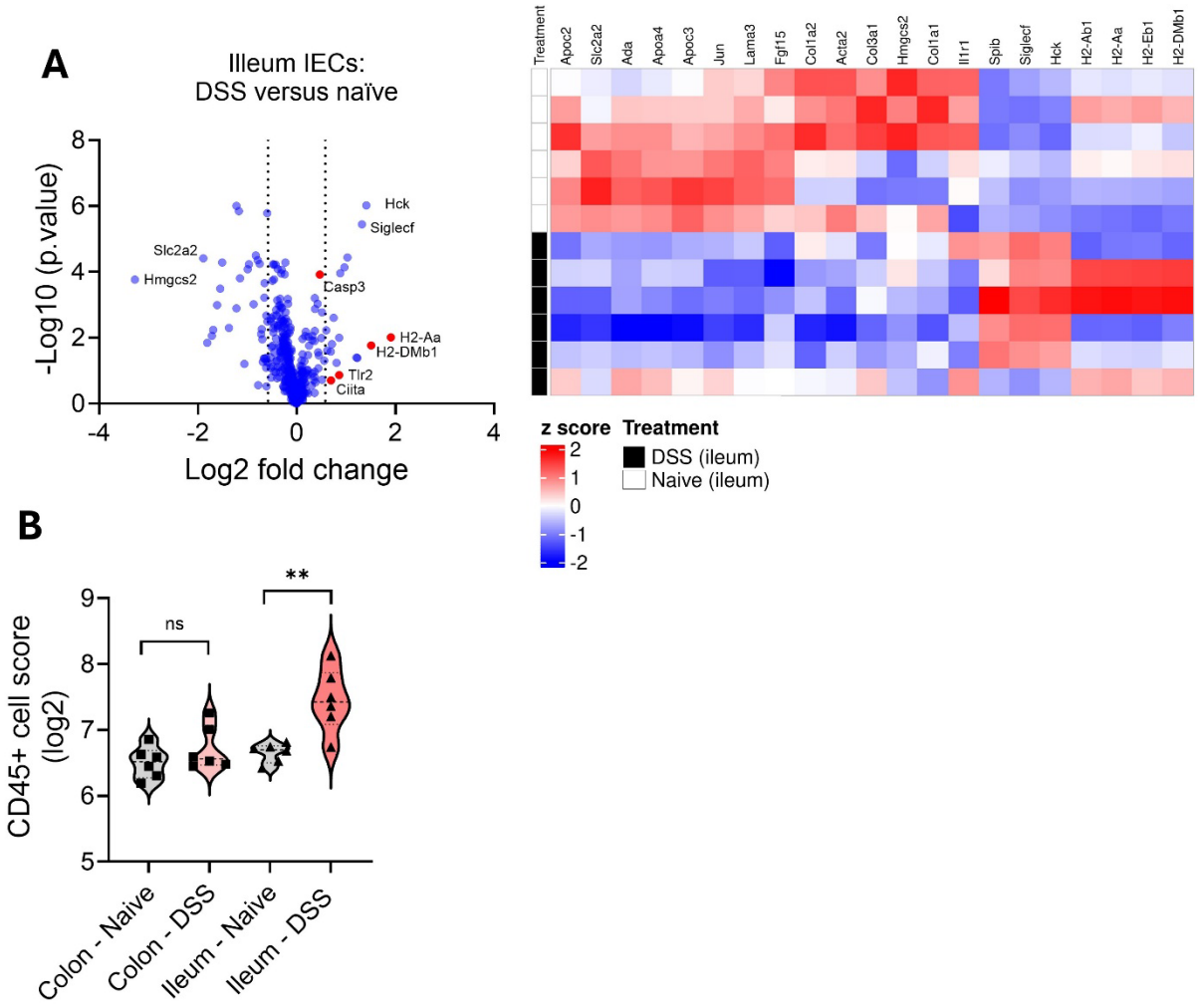
Supplemental Figure 11: Fecal occult blood is not the sole source of IgG in stool of IBD patients **(A)** Representative images of fecal occult blood test strips showing color change of strips in response to low, medium, or high blood content. **(B)** IgG content in IBD patient stool (both UC and CD) stratified by qualitative blood content. **(C)** Fecal IgG only considering IBD patients with no blood content in stool. Data is from the same donors shown in Figure 3. Points represent individual subjects; error bars represent mean ± s.e.m. Statistics are analyzed by Brown-Forsythe and Welch ANOVA with Dunnett's multiple comparisons test. ****$P < 0.0001$. LOQ: limit of quantification.



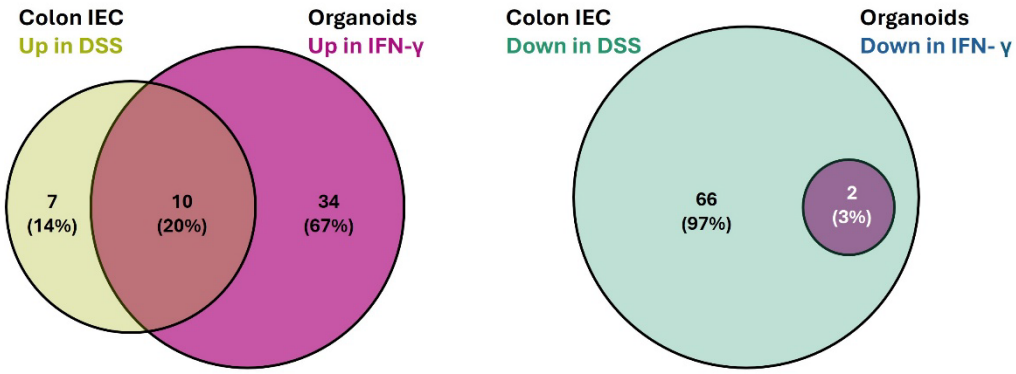
Supplemental Figure 12: Flow cytometry gating strategy for in vitro studies. **(A)** Gating strategy to identify plasmablasts and ABC-like plasmablasts with relevant FMO controls. **(B)** Representative flow cytometry gates from B cells stimulated with IFN-γ plus TLR7 agonist showing plasmablasts among CD19+ cells and ABCs among plasmablasts.



Supplemental Figure 13: ABCs are induced *in vitro* by stimulating with IFN-γ plus a TLR agonist or cecal contents. **(A)** Frequency of plasmablasts (PBs) and ABC-like PBs after 48h *in vitro* culture of isolated splenic or mesenteric lymph node (mLN) B cells in various stimuli analyzed by flow cytometry. TLR7 ag.: CL097; TLR5 ag.: recombinant flagellin; BCR: anti-IgM + anti-CD40. Gating strategy is shown in Supplemental Figure 12. **(B)** Concentration of TNF-α and IL-6 in culture supernatants analyzed by LegendPlex assay or MSD assay. **(C)** Frequency of activated B cells ($CD86^{+}MHC\text{-}II^{hi}$) and ABC-like PBs after 48h *in vitro* culture of isolated splenic B cells with IFN-γ plus cecal supernatants (sup.) generated from control mice. Cecal supernatants were added to B cell cultures at low (1:500) or high (1:50) concentration. Data in **A-B** is pooled from 3 independent experiments. Data in **C** is from 1 representative experiment of 2. Statistics are analyzed by two-way ANOVA **(A-B)** or one-way ANOVA (**C**) with Dunnett's multiple comparisons test against the unstimulated **(A, B)** or IFN-γ condition **(C)**. **P* < 0.05, ***P* < 0.01, ****P* < 0.001, *****P* < 0.0001. ns: nonsignificant. ULOD: upper limit of detection.

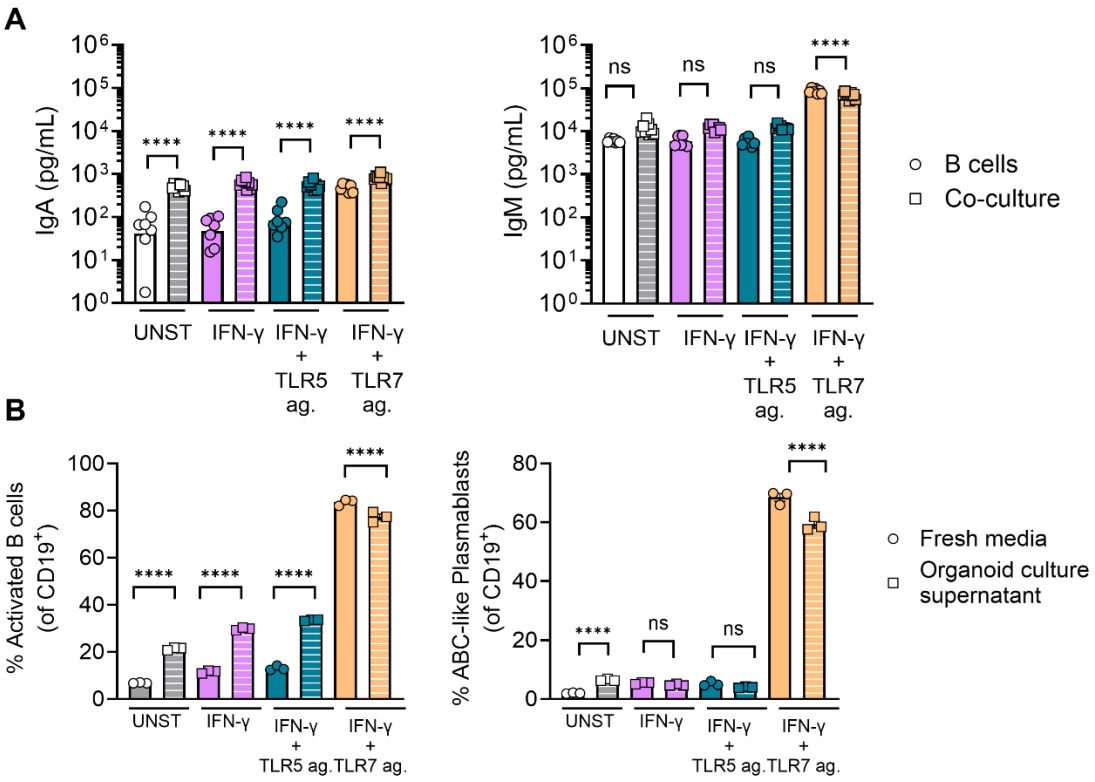


Supplemental Figure 14: Gene expression and immune cell contamination in crude epithelial cell preparation from naïve and DSS treated mice. **(A)** Volcano map of genes upregulated or downregulated in ileal intestinal epithelial cells (IECs) of DSS-treated mice compared to naïve. Genes of interest are marked in red. Differentially expressed genes are also represented in a heatmap, color corresponds to z score. **(B)** CD45+ cell score (log2 reduced transcript counts of *Ptprc*) in IEC cell preparations from the ileum and colon of naïve and DSS-treated mice. Data is from ileal IECs from the same experiment as Figure 4. Statistics in **B** are analyzed by Student's t test within each tissue (colon and ileum). $^{**}P < 0.01$. ns: nonsignificant.

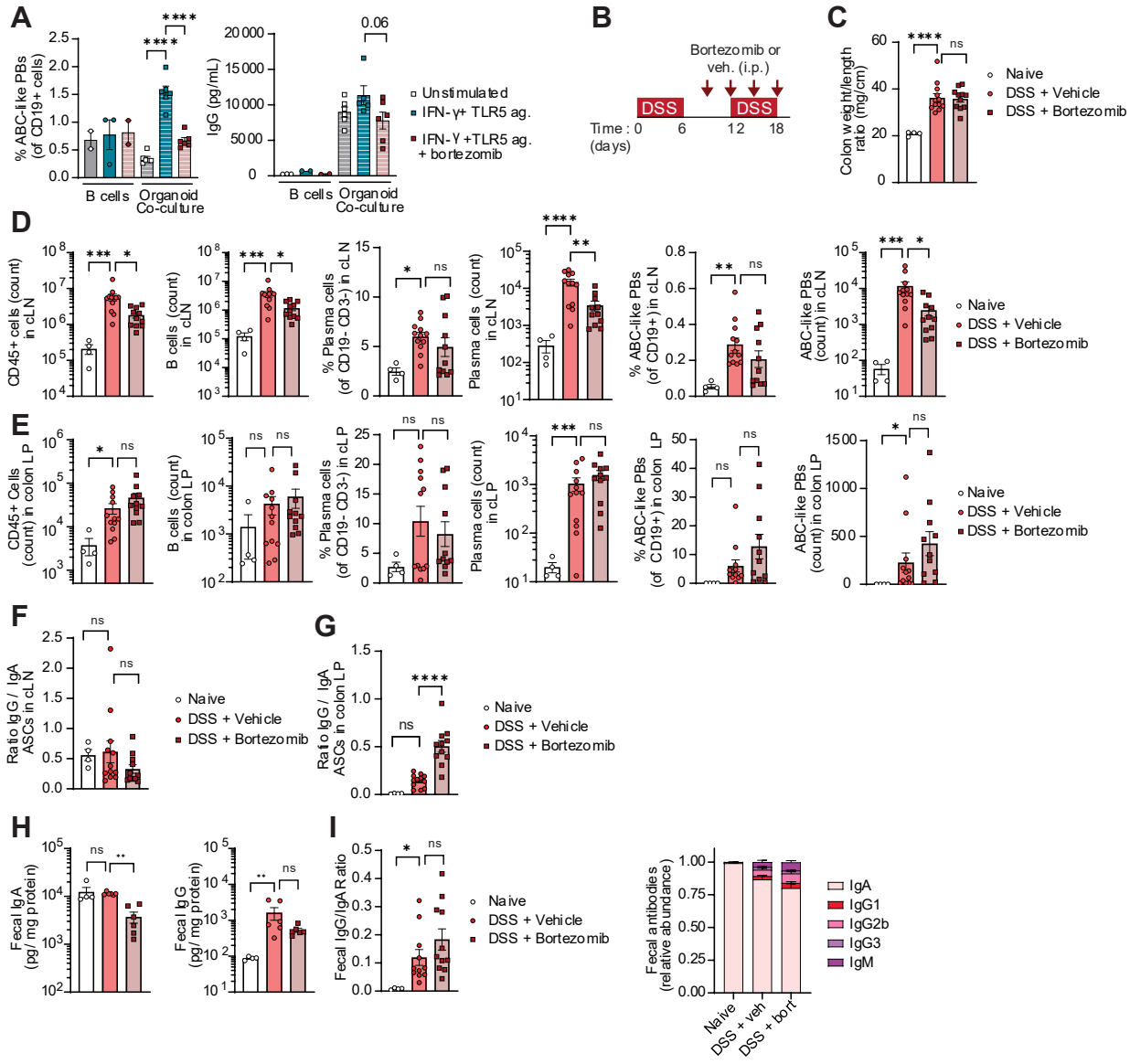


Gene	Full Name	Direction of Change Colon (DSS)	Direction of Change Organoid (IFN-γ)
Cxcl11	CXC Motif chemokine ligand 11 (I-TAC)	**UP**	**UP**
Ciita	Clas II Major Histocompatibility Complex Transactivator	**UP**	**UP**
Isg15	Interferon-Stimulated Gene 15	**UP**	**UP**
Psmb8	Proteasome 20S Subunit Beta (LMP7)	**UP**	**UP**
Stat1	Signal Transducer and Activator of Transcription 1	**UP**	**UP**
Tnfsf10	TNF Superfamily Member 10	**UP**	**UP**
Irf8	Interferon Regulatory Factor 8	**UP**	**UP**
Bst2	Bone Marrow Stromal Cell Antigen 2 (Tetherin)	**UP**	**UP**
Cd14	Cluster of Differentiation 14	**UP**	**UP**
Gpx2	Glutathione Peroxidase 2	**UP**	**UP**
Gab1	GRB2-Associated Binding Protein 1	**DOWN**	**DOWN**
Hmgcs2	3-Hydroxy-3-Methylglutaryl-CoA Synthase 2	**DOWN**	**DOWN**

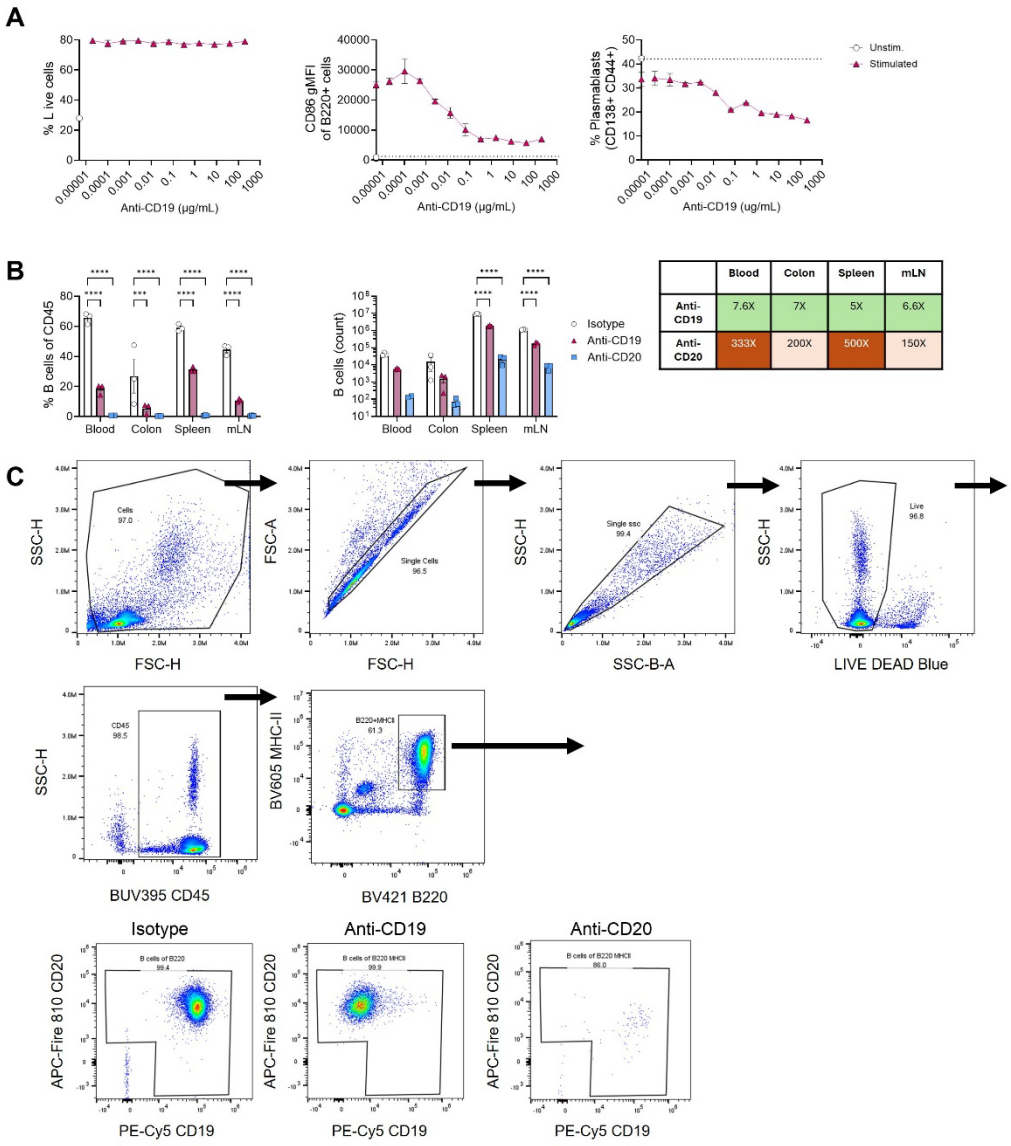
Supplemental Figure 15: Shared gene expression changes between *in vitro* and *in vivo* epithelial cells. The number of differentially expressed genes between damaged IECs (colon, DSS-treated) or stimulated organoids (organoids, IFN-γ) versus each untreated control are shown as circles. The overlap between circles shows the number of shared genes between each dataset. The names and functions of the shared genes are described in the table.



Supplemental Figure 16: Organoid co-culture significantly increases IgA production from co-cultured B cells. Conditioned media from stimulated intestinal organoids increases B cell activation compared to fresh media. **(A)** Total concentration of IgA and IgM in culture supernatants corresponding to Figure 5F. **(B)** Frequency of activated B cells ($CD86^{+}MHC\text{-}II^{hi}$) and ABC-like plasmablasts among total B cells after 48h culture in media supplemented with IFN-γ with or without a TLR5 or TLR7 agonist. Organoid culture supernatant was obtained from prior experiments in which organoids were stimulated for 48h as in Figure 4. Data in **A** is pooled from 3 independent experiments. Data in **B** is from 1 representative experiment. Points represent biological replicates, bars represent mean ± s.e.m. Statistics are analyzed by two-way ANOVA with Sidak's multiple comparisons test comparing fresh media versus organoid culture supernatant within each stimulation condition. $^{**}P < 0.01$, $^{****}P < 0.0001$. ns: nonsignificant. UNST: unstimulated.

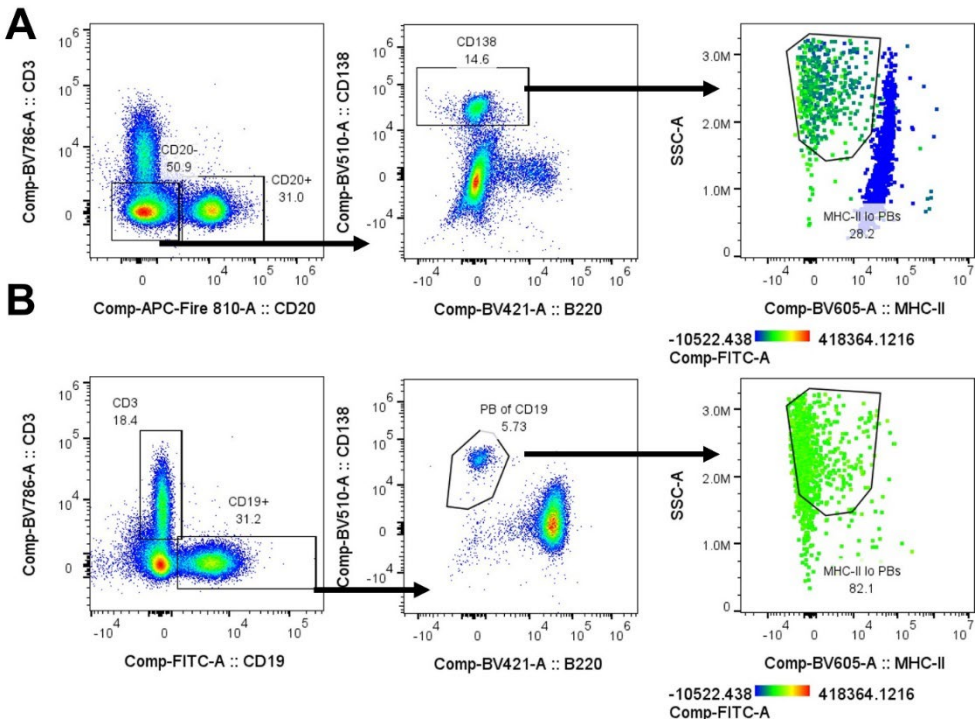


Supplemental Figure 17: Bortezomib inhibits ABC-like plasmablast induction *in vitro* and in the colon-draining lymph node of DSS-treated mice but does not impact colitis severity. **(A)** Isolated splenic B cells were cultured alone or co-cultured with intestinal organoids. Cultures were stimulated with IFN-γ plus a TLR5 agonist (flagellin), and some were supplemented with 50 pg/mL bortezomib. Controls received equal concentration of vehicle (0.001% DMSO). After 48h culture, the frequency of ABC-like plasmablasts (PBs) was measured by flow cytometry (left) and secreted IgG was measured by MSD assay (right). **(B)** Experimental timeline for chronic DSS model. Animals were treated with bortezomib (1mg/kg) or vehicle (1% DMSO) i.p. every 3 days beginning on day 9. **(C)** Disease severity measured by colon weight/length ratio. **(D-E)** Abundance of total CD45$^+$ cells, B cells, plasma cells, and ABC-like plasmablasts in the cecal-colonic lymph node (cLN, **D**) and colon lamina propria (LP, **E**) measured by flow cytometry. Cell populations are represented as total counts or percentages of parent population. **(F-G)** Ratio of the number of IgG secreting cells to IgA secreting cells in the cLN (**F**) and cLP (**G**) measured by ELISpot assay. **(H)** Concentration of IgA and IgG soluble antibody isotypes in feces. **(I)** The ratio of total IgG/ IgA concentration and relative abundance. Data in **A** is from 1 representative experiment, points represent biological replicates and bars represent mean ± s.e.m. Data in **B-I** is pooled from 2 independent experiments. Points represent individual mice and bars represent mean ± s.e.m. Data in (**A**) was analyzed by two-way ANOVA with Dunnett's multiple comparison's test against the stimulated control. Data in **C-I,** and cell frequencies in **D** were analyzed by one-way ANOVA with Dunnett's multiple comparison's test against the DSS + vehicle group. Cell counts in **D** and **F** were analyzed by Kruskal Wallis Test with Dunn's multiple comparisons test. *P < 0.05, **P < 0.01, ***P < 0.001, ****P < 0.0001. ns: nonsignificant.

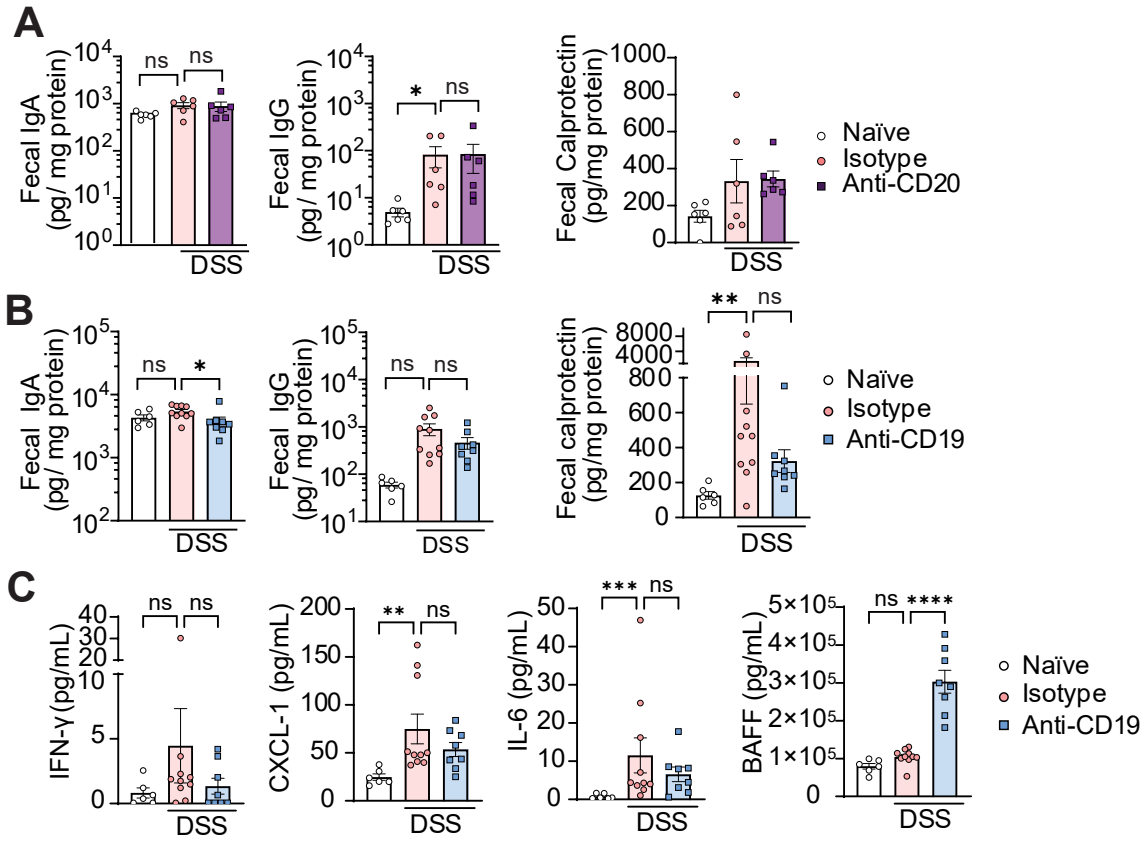


	Blood	Colon	Spleen	mLN
Anti-CD19	7.6X	7X	5X	6.6X
Anti-CD20	333X	200X	500X	150X

Supplemental Figure 18: Anti-CD19 antibody inhibits B cell activation *in vitro* but does not deplete B cells *in vivo*. **(A)** Isolated splenic B cells were cultured without stimulation or stimulated with anti-IgM plus anti-CD40 with ranging concentrations of anti-CD19 for 48h. Cell viability, activation (CD86), and plasmablast differentiation were analyzed by flow cytometry. Dotted lines show the unstimulated condition. Points on the y axis are from wells with zero anti-CD19. **(B)** B cell frequency and cell count in various tissues from mice treated with anti-CD19, anti-CD20 or isotype control. Average B cell count reduction compared to isotype control within each tissue is shown in the table. WT C57BL/6 mice were treated i.p. with 10mg/kg anti-CD19 or isotype control every six days for 3 doses. Tissues were collected 48h after the last dose and B cell populations (CD3- B220+ MHC-II+) were analyzed by flow cytometry. **(C)** Flow cytometry gating strategy and representative plots of B cells (CD3- B220+ MHC-II+) in the blood showing depletion with anti-CD20 and CD19 blocking with anti-CD19. Data shown in **A** and **B** are each from 1 representative experiment of 2. In **A**, points represent the average value from *n* = 2 biological replicates, error bars represent the mean ± s.e.m. In **B**, points represent individual mice, bars represent the mean ± s.e.m. Statistics were analyzed by two-way ANOVA with Sidak's multiple comparisons test. ****$P < 0.0001$.



Supplemental Figure 19: Plasmablast gating strategy related to Figure 6L. **(A)** Example gating strategy to define plasmablasts in experiments utilizing CD19 blocking antibody in vivo (Figure 6 H-M). Plasmablasts were defined as CD20- CD138+ SSCA^{hi} MHC-II^{low}. Color intensity on the final panel shows CD19 expression on the gated population. **(B)** Gating strategy was confirmed by gating CD19+ CD138+ plasmablasts as in previous experiments. Within the CD19+ CD138+ gate, the majority of cells fall within the SSC-A^{hi} MHC-II^{low} gate. Representative plots are from an isotype-treated mouse.



Supplemental Figure 20: B cell blocking antibody treatment does not significantly reduce fecal biomarkers or serum cytokines in DSS-treated mice. **(A, B)** Fecal IgA, IgG, and calprotectin measured by MSD assay or ELISA. **(C)** Serum cytokines measured on day 20 by LegendPlex assay. Statistics were analyzed by lognormal one-way ANOVA with Dunnett's multiple comparison's test against the DSS isotype group. *$P < 0.05$, **$P < 0.01$, ***$P < 0.001$****, $P < 0.0001$. ns: nonsignificant.

Supplemental Table 1: Patient demographic information. Demographic information and treatment history of Crohn's disease patients related to data in Figure 1.

Patient #	Age	Sex	Race	Age of Dx	Disease location	Phenotype	Current treatments	Prior treatments	Surgery
1	20	F	Caucasian	12	Ileocolonic	Stricturing	Adalimumab	Infliximab	Ileocolonic resection
2	24	M	Asian	20	Ileal	Penetrating	Adalimumab	none	Small bowel resection
3	36	M	Caucasian	16	Ileocolonic	Penetrating	None	Infliximab	Ileocolonic resection
4	29	F	Caucasian	27	Ileal	Stricturing	Ustekinumab	Adalimumab, ustekinumab	Ileocolonic resection, stricturoplasty
5	32	M	Caucasian	14	Ileal	Penetrating	Infliximab	adalimumab, ustekinumab	Ileocolonic resection
6	19	F	Caucasian	14	Ileocolonic	Stricturing	Infliximab	none	Ileocolonic resection
7	48	M	Middle Eastern	44	Ileal	Stricturing	Ustekinumab	Infliximab, adalimumab	Ileocolonic resection
8	51	M	Caucasian	22	Ileocolonic	Penetrating	Ustekinumab	Infliximab, adalimumab	Ileocolonic resection

Supplemental Table 2: CITESeq antibodies related to Figure 1.

Antibody Name and Target	Antibody Name and Target	Antibody Name and Target
TotalSeq™-A0145 anti-human CD103 (Integrin αE) Antibody	TotalSeq™-A0148 anti-human CD197 (CCR7) Antibody	TotalSeq™-A0176 anti-human CD39 Antibody
TotalSeq™-A0155 anti-human CD107a (LAMP-1) Antibody	TotalSeq™-A0100 anti-human CD20 Antibody	TotalSeq™-A0072 anti-human CD4 Antibody
TotalSeq™-A0061 anti-human CD117 (c-kit) Antibody	TotalSeq™-A0152 anti-human CD223 (LAG-3) Antibody	TotalSeq™-A0073 anti-mouse/human CD44 Antibody
TotalSeq™-A0014 anti-mouse/human CD11b Antibody	TotalSeq™-A0189 anti-human CD244 (2B4) Antibody	TotalSeq™-A0048 anti-human CD45 Antibody
TotalSeq™-A0053 anti-human CD11c Antibody	TotalSeq™-A0085 anti-human CD25 Antibody	TotalSeq™-A0103 anti-mouse/human CD45R/B220 Antibody
TotalSeq™-A0064 anti-human CD123 Antibody	TotalSeq™-A0191 anti-mouse/rat/human CD27 Antibody	TotalSeq™-A0063 anti-human CD45RA Antibody
TotalSeq™-A0390 anti-human CD127 (IL-7Rα) Antibody	TotalSeq™-A0171 anti-human/mouse/rat CD278 (ICOS) Antibody	TotalSeq™-A0087 anti-human CD45RO Antibody
TotalSeq™-A0158 anti-human CD134 (OX40) Antibody	TotalSeq™-A0088 anti-human CD279 (PD-1) Antibody	TotalSeq™-A0575 anti-human CD49a Antibody
TotalSeq™-A0022 anti-human CD137L (4-1BB Ligand) Antibody	TotalSeq™-A0386 anti-human CD28 Antibody	TotalSeq™-A0576 anti-human CD49d Antibody
TotalSeq™-A0831 anti-human CD138 (Syndecan-1) Antibody	TotalSeq™-A0369 anti-human CD29 Antibody	TotalSeq™-A0047 anti-human CD56 (NCAM) Antibody
TotalSeq™-A0081 anti-human CD14 Antibody	TotalSeq™-A0102 anti-human CD294 (CRTH2) Antibody	TotalSeq™-A0147 anti-human CD62L Antibody
TotalSeq™-A0392 anti-human CD15 (SSEA-1) Antibody	TotalSeq™-A0034 anti-human CD3 Antibody	TotalSeq™-A0560 anti-mouse CD68 Antibody
TotalSeq™-A0083 anti-human CD16 Antibody	TotalSeq™-A0406 anti-human CD304 (Neuropilin-1) Antibody	TotalSeq™-A0146 anti-human CD69 Antibody
TotalSeq™-A0149 anti-human CD161 Antibody	TotalSeq™-A0165 anti-human CD314 (NKG2D) Antibody	TotalSeq™-A0005 anti-human CD80 Antibody
TotalSeq™-A0140 anti-human CD183 (CXCR3) Antibody	TotalSeq™-A0830 anti-human CD319 (CRACC) Antibody	TotalSeq™-A0006 anti-human CD86 Antibody
TotalSeq™-A0366 anti-human CD184 (CXCR4) Antibody	TotalSeq™-A0135 anti-human CD324 (E-Cadherin) Antibody	TotalSeq™-A0080 anti-human CD8a Antibody
TotalSeq™-A0144 anti-human CD185 (CXCR5) Antibody	TotalSeq™-A0123 anti-human CD326 (Ep-CAM) Antibody	Possibly Purified anti-human CD8b Recombinant Antibody
TotalSeq™-A0804 anti-human CD186 (CXCR6) Antibody	TotalSeq™-A0360 anti-human CD357 (GITR) Antibody	TotalSeq™-A0060 anti-human CD90 (Thy1) Antibody
TotalSeq™-A0050 anti-human CD19 Antibody	TotalSeq™-A0169 anti-human CD366 (Tim-3) Antibody	TotalSeq™-A0867 anti-human CD94 Antibody
TotalSeq™-A0143 anti-human CD196 (CCR6) Antibody	TotalSeq™-A0410 anti-human CD38 Antibody	TotalSeq™-A0179 anti-human CX3CR1 Antibody
TotalSeq™-A0159 anti-human HLA-DR Antibody	TotalSeq™-A0136 anti-human IgM Antibody	TotalSeq™-A0214 anti-human/mouse integrin β7 Antibody
TotalSeq™-A0250 anti-mouse/human KLRG1 (MAFA) Antibody	TotalSeq™-A0584 anti-human TCR Vα24-Jα18 (iNKT cell) Antibody	TotalSeq™-A0581 anti-human TCR Vα7.2 Antibody
TotalSeq™-A0224 anti-human TCR α/β Antibody	TotalSeq™-A0139 anti-human TCR γ/δ Antibody	TotalSeq™-A0089 anti-human TIGIT (VSTM3) Antibody

Supplemental Table 3: Flow cytometry antibodies.

Marker	Fluorophore	Vendor	Catalogue #	Clone
Anti-mouse CD45	BUV 395	Invitrogen	363-0451-82	30-F11
Anti-mouse CD86	BUV737	BD	741737	GL1
Anti-mouse CD4	BUV805	BD	741912	RM4-5
Anti-mouse B220	BV421	BD	BDB562922	RA3-6B2
Anti-mouse CD138	BV510	BD	BDB563192	281-2
Anti-mouse MHCII (I-A/I-E)	BV605	BD	563413	M5/114.15.2
Anti-mouse CD3	BV786	Invitrogen	417-0031-82	145-2C11
Anti-mouse CD19	FITC	BD	BDB557398	1D3
Anti-mouse GL7	PerCP-Cy5.5	BioLegend	50-605-095	GL7
Anti-mouse CD11b	APC	BD	BDB553312	M1/70
Anti-mouse CD44	AF 700	BD	560567	1M7
Anti-mouse CD11c	APC-Cy7	BD	561241	HL3
Anti-mouse CD20	APC-Fire 810	BioLegend	150438	SA275A11
Anti-mouse/human T-bet	PE	Invitrogen	50-112-9387	4B10
Anti-mouse CD19	PE-Cy5	Invitrogen	35-0193-82	1D3
Anti-human CD3	BUV395	BD	563546	UCHT1
Anti-human CD11c	BV421	BD	566877	BU15
Anti-human CD20	BV786	BioLegend	302356	2H7
Anti-human CD19	FITC	BioLegend	302206	HIB19
Anti-human Blimp1	AF647	R&D Systems	IC36081R	646702

Supplemental Table 4: Barcoded antibodies and reporters for immunofluorescent imaging.

Marker / Barcode	Reporter Fluorophore	Vendor	Antibody Catalogue #	Clone
Anti-mouse CD20-BX064	AF488 RX064	Akoya	Custom	
Anti-mouse CD90.2-BX001	AF488 RX001	Akoya	4150001	30-H12
Anti-mouse B220-BX010	AF488 RX010	Akoya	4150006	Ra3-6B2
Anti-mouse CD45-BX007	AF488 RX007	Akoya	4150002	30-F11
Anti-mouse MHC-II-BX014	Atto 550 RX014	Akoya	4250003	M5/114.15.2
Anti-mouse CD19-BX020	Atto 500 RX020	Akoya	4250014	6D5
Anti-mouse CD4-BX026	Atto 550 RX026	Akoya	4250016	RM4-5
Anti-mouse CD8a-BX029	Atto 550 RX029	Akoya	4250017	53-6.7
Anti-mouse CD11C-BX030	AF647 RX030	Akoya	4550108	N418
Anti-mouse CD3-BX021	AF647 RX021	Akoya	4550109	17A2
Anti-mouse EpCAM-050	AF647 RX050	BioLegend	118201	G8.8